Science Advances
AAAS

Supplementary Materials for

Single-synapse analyses of Alzheimer's disease implicate pathologic tau, DJ1, CD47, and ApoE

Thanaphong Phongpreecha, Chandresh R. Gajera, Candace C. Liu, Kausalia Vijayaragavan, Alan L. Chang, Martin Becker, Ramin Fallahzadeh, Rosemary Fernandez, Nadia Postupna, Emily Sherfield, Dmitry Tebaykin, Caitlin Latimer, Carol A. Shively, Thomas C. Register, Suzanne Craft, Kathleen S. Montine, Edward J. Fox, Kathleen L. Poston, C. Dirk Keene, Michael Angelo, Sean C. Bendall, Nima Aghaeepour, Thomas J. Montine*

*Corresponding author. Email: tmontine@stanford.edu

Published 15 December 2021, *Sci. Adv.* **7**, eabk0473 (2021)
DOI: 10.1126/sciadv.abk0473

This PDF file includes:

SUPPLEMENTARY TEXT

Preliminary robustness and cluster sanity checks of the clusters

To ensure that the resulting clusters were robust, a leave-one-out cluster prediction was performed on the Control samples and compared to the original results obtained from training on all 6 Control samples. Specifically, in each of the 6 iterations, the autoencoder was trained on 5 Control samples and predicted the cluster assignment for the held-out sample. The results are visualized in **Fig. S2B**, where each pixel of the heatmap represents average scaled expression values from the predicted held-out samples. The similarity between this heatmap and that in Fig. 2A suggests that the resulting clusters are equivalent. The mean and standard deviation of the correlation statistics (Pearson's R) between them for each of the phenotypic markers are shown on the left of the heatmap.

Autoencoder-generated clusters were initially validated by two approaches. First, subpopulations followed prior expectations, *e.g*, all presynaptic subpopulations in caudate exhibited multiple fold higher DAT expression than in BA9 or hippocampus (**Fig. S9**). Second, the intentionally selected redundant presynaptic markers, CD47 and SNAP25, had highly correlated signal intensities across subpopulations (Spearman's R=0.90, 0.91, and 0.91 in BA9, caudate, and hippocampus, $P=2.2\times10^{-16}$ for all regions). We and others *(16, 64, 65)* have shown that a minority of synaptosomes retain attached astrocytic components*;* the intentionally redundant astrocytic markers, EAAT1 and GFAP, exhibited strong correlations of intensities across multiple subpopulations in all regions (Spearman's R=0.74, 0.62, and 0.68 in BA9, caudate, and hippocampus, $P<2.2\times10^{-16}$ for all regions).

SUPPLEMENTARY FIGURES

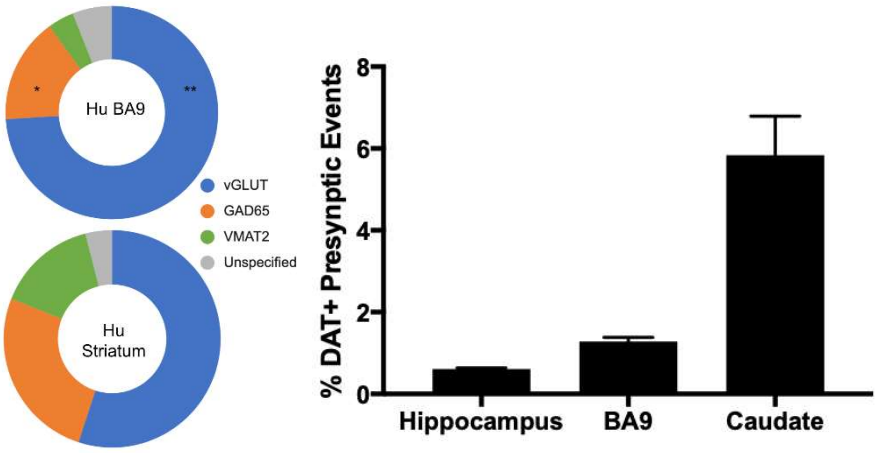

Fig. S1. Comparison of the SynTOF % positive events to known ultrastructural studies indicates good agreement. Ultrastructural studies have estimated the proportion of different types of synapses in primate brain. In prefrontal cortex, approximately 80% of synapses are ultrastructurally asymmetric, of which 85-90% are glutamatergic, aligning well with our SynTOF estimate of 73.0±3.5% BA9 vGLUT+ synaptosomes in Controls *(21)*. The approximately 20% symmetric synapses in prefrontal cortex are mostly GABAergic, estimated at 1 in 6, or 17% of total *(21)*. The percent of BA9 GAD65+ presynaptic events by SynTOF was 16.3±1.4% in Controls. The remaining symmetric synapses (about 3% of total) and some of the non-glutamatergic asymmetric synapses are monoaminergic, both noradrenergic and dopaminergic at this site, although ultrastructural assessments of monoaminergic terminals are likely underestimates because many terminals are not well formed synapses *(22,23)*. BA9 VMAT2+ events were 4.3±0.9% of Control total presynaptic events by SynTOF. In primate caudate nucleus, 70% to 86% of synapses are asymmetric but only two-thirds, or 47% to 58%, are glutamatergic *(24)*. Control caudate vGLUT+ presynaptic events were 55.0±1.5% of total by SynTOF, which was significantly less than in BA9 (**P<0.01). The remaining asymmetric synapses in caudate are mostly serotonergic with some dopaminergic. Symmetric synapses in the caudate nucleus range from 24% to 30% and are mostly GABAergic along with dopaminergic *(24, 25)*. Control caudate GAD65+ presynaptic events were 26.2±1.6%, by SynTOF, which was significantly more than BA9 (*P<0.05). VMAT2+ presynaptic events in Control caudate were 14.5±2.6% of total by SynTOF. The ratio of DAT to VMAT2 varies between 0.5 and 0.3 in human striatum *(27)*. DAT+/VAMT2+ presynaptic events by SynTOF averaged 0.4 in Controls. As expected, distribution of DAT+ presynaptic events by SynTOF was significantly different across the three regions in Controls (P<0.0001) with caudate approximately 5-fold greater than BA9 (P<0.001) and 10-fold greater than hippocampus *(27)* (P<0.001).

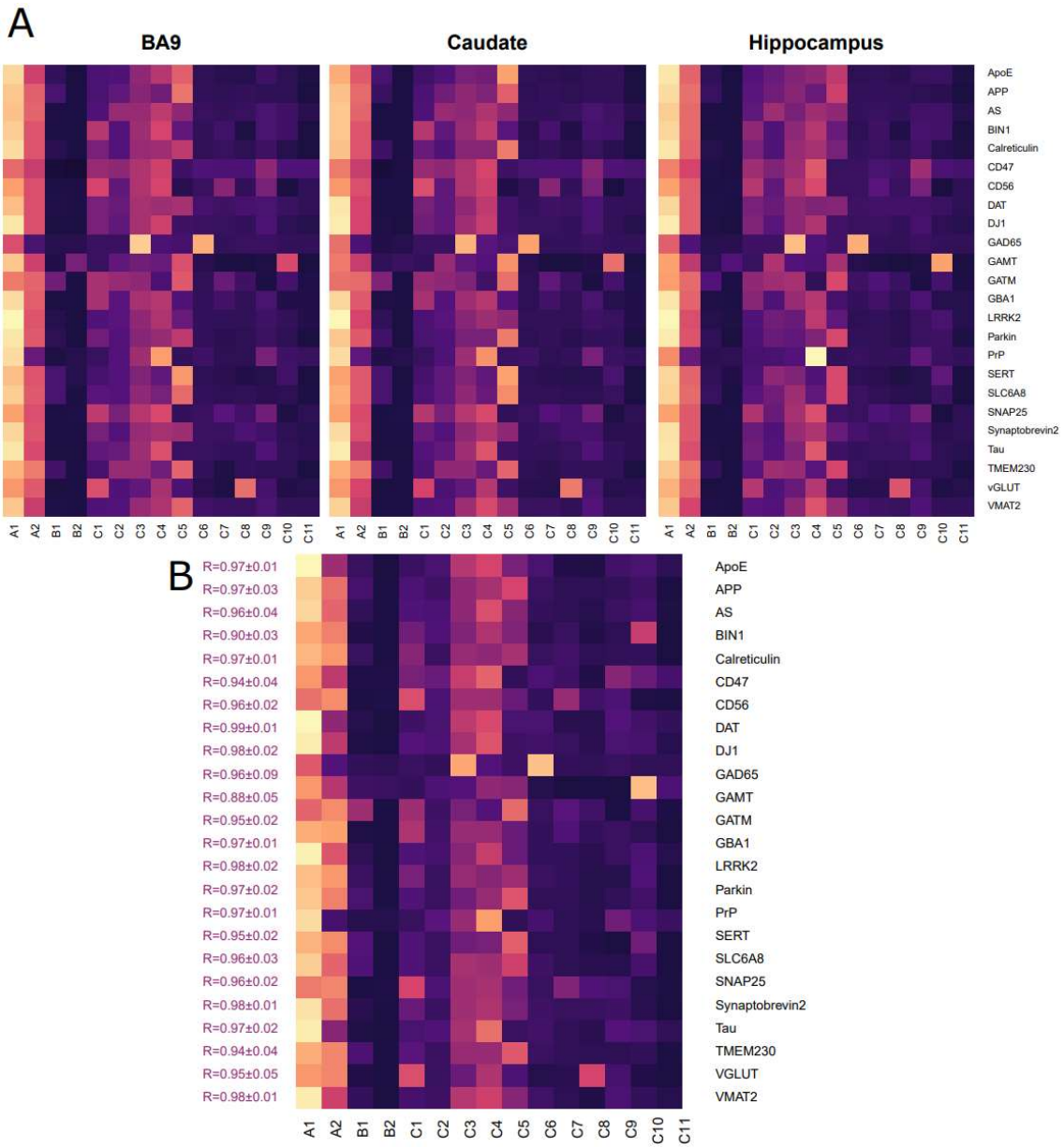

Fig. S2. Heatmaps of mean expression for phenotypic markers in each brain region and from a leave-one-out clustering robustness analysis. (**A**) Heatmap showing the mean expression values from Control samples for each of the phenotypic markers across all identified subpopulations and stratified by brain region. The mean expression values were scaled across subpopulations for differential visualization purposes. These heatmaps demonstrate that the subpopulation characteristics were similar across all brain regions. (**B**) Heatmap showing the mean expression values from the average of the leave-one-out prediction of the six Control samples (all brain regions). For each of the phenotypic markers, the correlations to the mean expression values obtained from training and predicting using all six samples (as shown in Fig. 2A) were measured by Pearson's R. The high correlations between the two indicate the robustness of the clustering results. The mean expression values were scaled across subpopulations for visualization purposes.

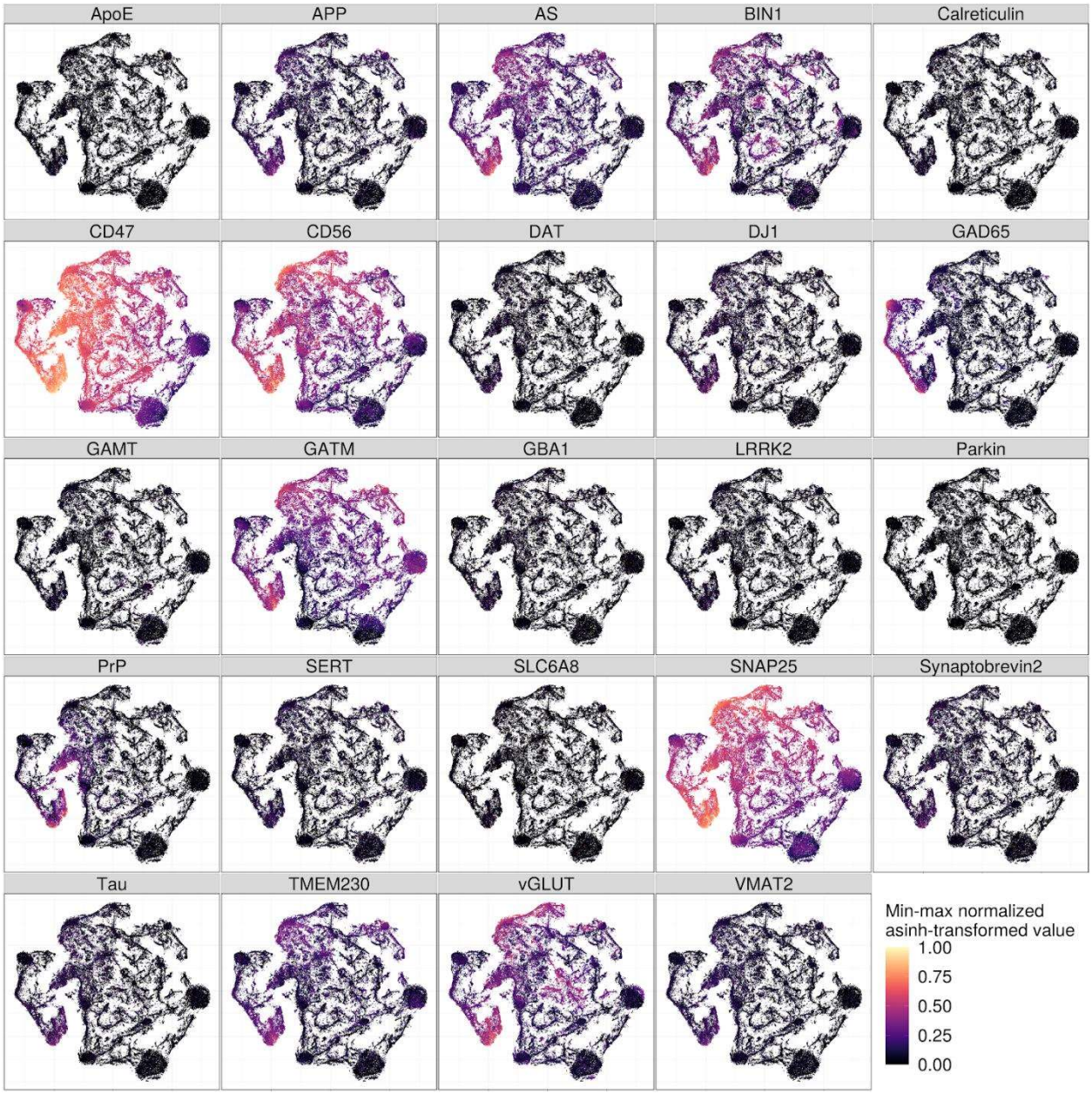

Fig. S3. **A 2-D t-SNE projections colored by phenotypic intensity confirm phenotypic definitions of each subpopulation.** The t-SNE plot of the sampled autoencoder's hidden representations from all brain regions of the Control samples with each event colored by the intensity of each of the defined phenotypic markers.

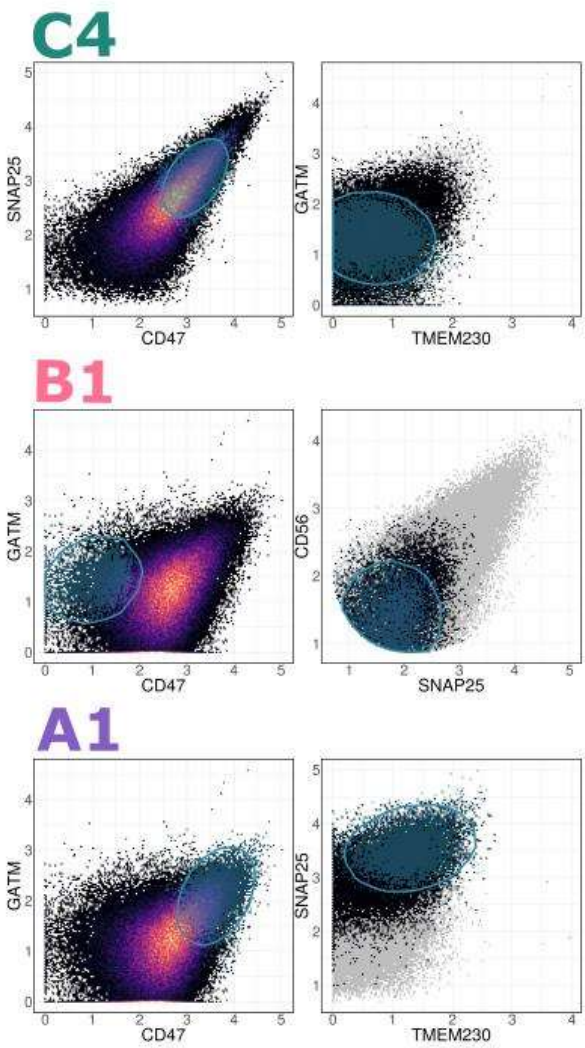

Fig. S4. Visualization of gated subpopulations. Biaxial plots obtained from GateFinder showing selected examples of subpopulations from samples in the BA9 region (A1, B1, and C4). The black-to-yellow color scale represents the density of the events; gray represents events that were excluded by the previous gating step.

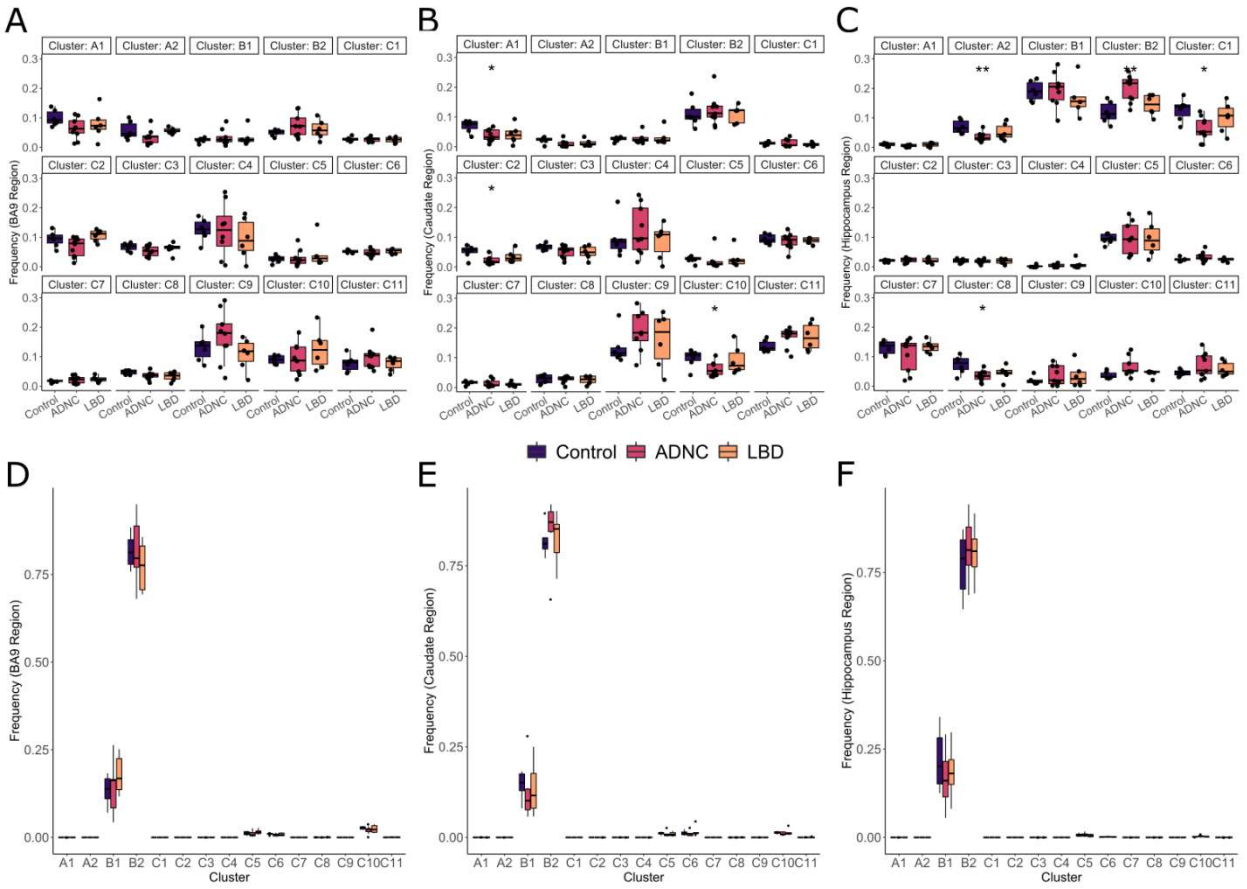

Fig. S5. **Pre- and postsynaptic subpopulation frequenciesy across all regions and diagnoses show little difference between diagnoses and postsynaptic events occurring mostly in B subpopulations.** (**A**)-(**C**) The frequency of each subpopulation of presynaptic events for Control, ADNC, and LBD in BA9, caudate, and hippocampus region, respectively. Asterisks indicate that the frequency of the disease group is significantly different (Wilcoxon) from Control. (**D**)-(**F**) The frequency of each subpopulation of postsynaptic events for Control, ADNC, and LBD in BA9, caudate, and hippocampus region, respectively. Most postsynaptic events were similar to subpopulation B.

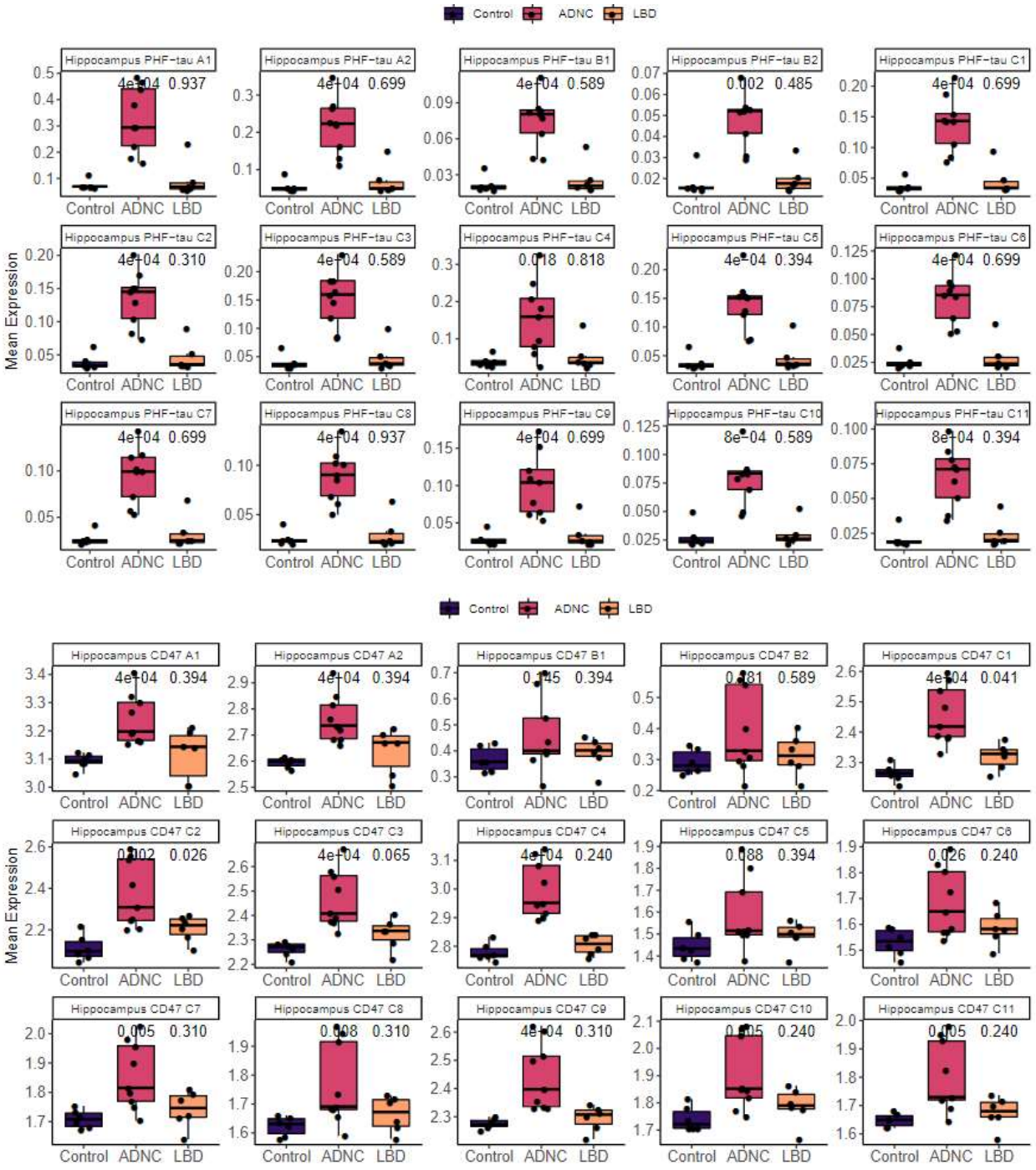

Fig. S6. **Expression of markers with separation between Control and AD groups in the majority of subpopulations.** These include PHF-tau expression for almost all subpopulations in hippocampus (top) and CD47 expression for most subpopulations with higher CD47 expressions in hippocampus (bottom), including subpopulation A1 and A2, C1to C4, and C7 to C11. Numbers above the bars for ADNC and LBD indicate Wilcoxon's P values for disease groups compared to Control.

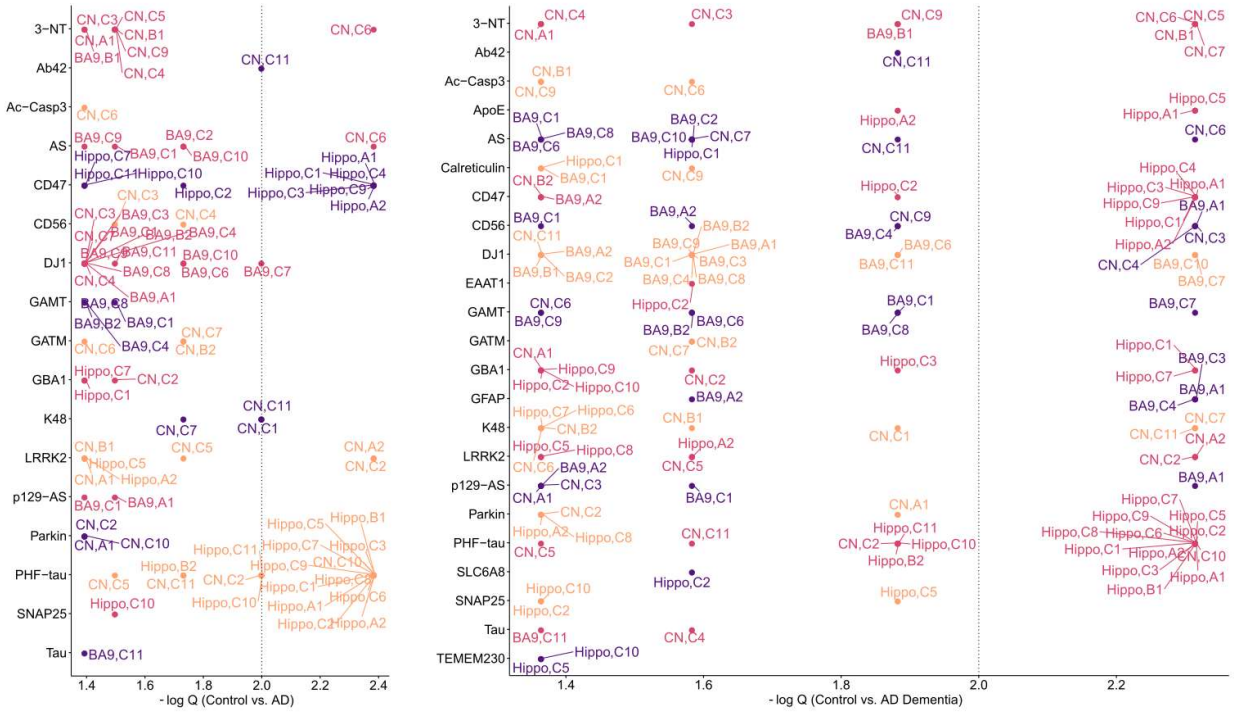

Fig. S7. **The tabulated list of all significant features between Control vs. AD and Control vs. AD Dementia.** The list of all significant features (Q value < 0.05) from Spearman's correlation for Control (n=6) vs. AD (n=9) (left) stratified by marker type shows prevalent and strong signals from PHF-tau and CD47 expression in multiple hippocampal subpopulations. Less strong, but still prevalent expression signals are DJ1 in multiple BA9 subpopulations. Other notable signals include GATM and K48 in caudate, and 3-NT in BA9. The right panel shows a list of all significant features (Q value < 0.05) for Control (n=6) vs. AD dementia (n=7), in which most signals from the previous comparison became stronger. Notably, ApoE was one of the few new signals (absent in the left panel) that also ranked among the strongest. Markers omitted on the y-axis were those without any significant subpopulations in any brain regions. Color is included only to facilitate visualization of each row. Note that CN and Hippo are abbreviations for caudate and hippocampus, respectively.

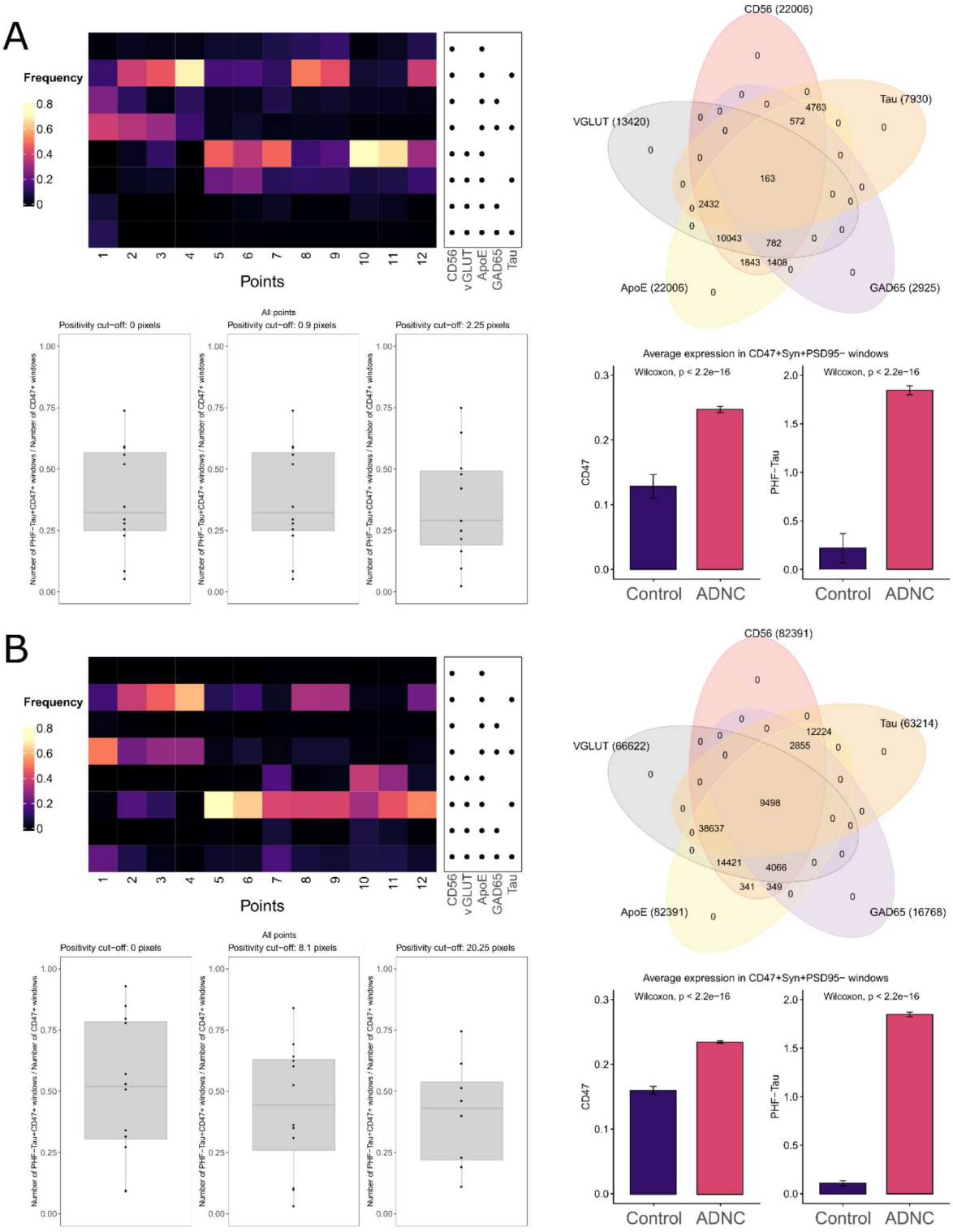

Fig. S8. Similar MIBI analyses to Fig. 5 but with different sliding window sizes resulted in the same conclusions. (**A**) Analyses using a window size of 3×3 (0.9 μm^2) and (**B**) 9×9 pixels (2.7 μm^2).

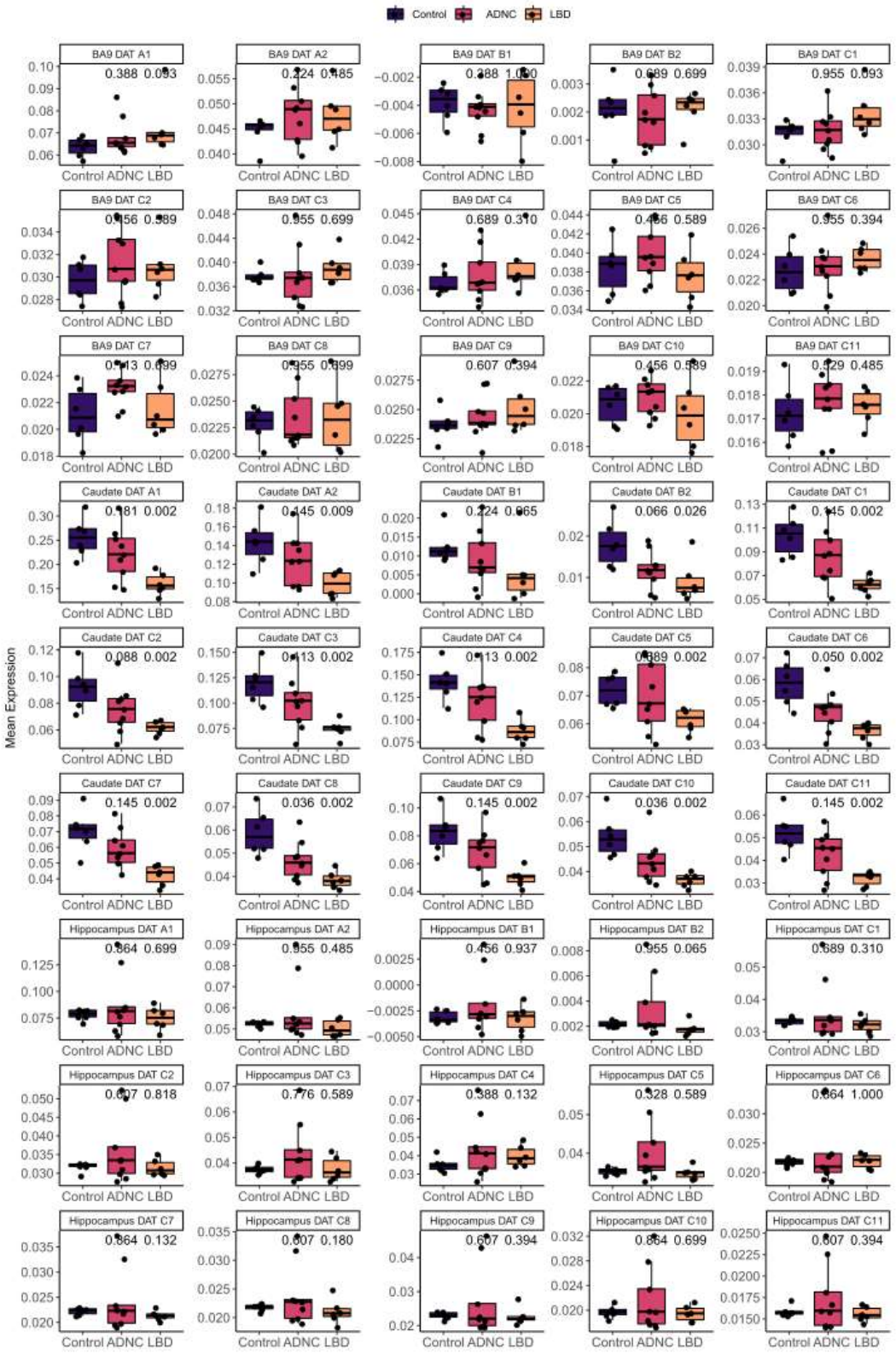

Fig. S9. **DAT expression in all subpopulations and regions conforms with prior expectations.** In particular, DAT expression was several folds higher in the caudate nucleus.

SUPPLEMENTARY TABLES

Table S1. Characteristics of Human Samples.

Group			**Control**	**ADNC**	**LBD**
N			6	9	6
Age (yr, mean ± SD)			86 ± 8	88 ± 7	88 ± 6
Sex (F:M)			1:2	2:1	1:1
Clinical Diagnosis	**Cognitively Normal (N)**		6	2	2
	MCI (N)		0	1	1
	Dementia (N)		0	6	3
PMI (hr, mean ± SD)			4.9 ± 1.6	5.0 ± 1.9	5.0 ± 0.8
Brain (gm, mean ± SD)			1182 ± 84	1084 ± 72	1260 ± 145
Pathologic features^	**ADNC (N)**	**No**	2	0	3
		Low	4	0	3
		Intermediate	0	0	0
		High	0	9	0
	LB (N)	**None**	6	9	0
		Brainstem	0	0	0
		Limbic	0	0	1
		Neocortical	0	0	5
	VBI (N)		None	None	None

	HS (N)	None	None	None
	TDP-43(N)	None	None	None
	ARTAG (N)	None	None	None
	CTE (N)	None	None	None

^Research participants who consented to brain autopsy with post mortem interval (PMI) < 8 hr had brain regions immediately processed and cryopreserved for synaptosomes as previously described *(16, 17, 35)*. Regions included Brodmann area (BA) 9 of the prefrontal cortex, hippocampus at the level of the lateral geniculate nucleus, and dorsolateral caudate nucleus. Over 5 years we collected samples from 113 brain autopsies, and included all who met the stringent clinical and pathological criteria detailed below. These criteria were established prior to selection in order to focus on cases with only one type of pathologic change: all cases that met these criteria were included in the study. Individuals in the **Control** group were cognitively normal at their last clinical evaluation, which was within 2 years of death, and had cognitive test results that were in the upper three quartiles for the cohort to minimize the likelihood of interval conversion. Neuropathologic evaluation of Control individuals (n=6) had no or low AD neuropathologic change (ADNC) and no comorbidities. Individuals in the **ADNC** group (n=9) all had neuropathologic evaluations that showed only high ADNC and no evidence of any comorbidity; they were clinically diagnosed as AD dementia (n=7) or cognitively normal (n=2) or as mild cognitive impairment (n=1) within 2 years of death. Individuals in the Lewy body (LB) disease (**LBD**) group (n=6) had only limbic or neocortical LB and were clinically diagnosed as cognitively normal within 2 years of death (n=2), Parkinson's disease (PD) with MCI or dementia (n=2), or Dementia with Lewy bodies (DLB) (n=2).

Table S2. **SynTOF antibody panel.** Our SynTOF panel contained 38 conjugated antibodies. For convenience antibodies were grouped into Marker Type (Fig. 1) used to identify features of cell type, synapse type, patho-physiological protein in synapse, protein products of several AD or PD risk genes, and markers of injury/response to injury. For quality control and normalization, we used EQ™ Four Element Calibration Beads (Fluidigm #201078), which have a unique 140Ce tag, and Cell ID™ Intercalator (191 Ir for DNA1 and 193 Ir for DNA2).

	Antibody	Descriptor	Product identifier	Clone	Metal tag	Synaptic / Phenotypic Marker
Gating	CD11b*	microglia	Fluidigm # 3148003B	M1/70	148 Nd	N/N
	MBP*	oligodendroglia	Biolegend # 808402	SMI 99	150 Nd	N/N
	CD56	pan-neuron	Fluidigm # 3163007B (Hu) Novus # MAB7820 (Mu)	NCAM16.2 (Hu) 809220 (Mu)	163 Dy	Y/Y
	SNAP25	pre-synaptic	Biolegend # 836304	SMI 81	155 Gd	Y/Y
	PSD95*	post-synaptic	Biolegend # 810401	K28/43	157 Gd	N/N
	Gephyrin*	post-synaptic	Synaptic Sys # 147011	mAb7	145 Nd	N/N
Neuron type	CD47	pre-synaptic	BioXcell/inVivomab # BE0283	MIAP410	151 Eu	Y/Y
	PrP	pan-neuronal	Biolegend # 800302	3F4	166 Er	Y/Y
	VGLUT	excitatory	Biolegend# 821301/ SySy # 135411	N28-9/321A8	153 Eu	Y/Y
	AS	pre-synaptic	Biolegend # 807702	LB509	142 Nd	Y/Y
	Tau	neuron	Millipore Sigma # MABN162	TAU-5	172 Yb	Y/Y

			(Aka MAB361, unpurified)			
	APP	neuron	Invitrogen # 14-9749-82	22C11	173 Yb	Y/Y
	GAD65	inhibitory	Biolegend # 844502	N-GAD65	169 Tm	Y/Y
	Calreticulin	pre-synaptic/phagocytosis	Enzo # ADI-SPA-601-F	FMC 75	162 Dy	Y/Y
	Synaptobrevin2	pre-synaptic	Synaptic Sys # 104211	69.1	115 In	Y/Y
	VMAT2	monoaminergic	Abcam # ab191121	poly	113 In	Y/Y
	SERT	serotonergic	Millipore Sigma # SAB2500950	poly	175 Lu	Y/Y
	DAT	dopaminergic	Abcam # ab5990	hDAT-NT	154 Sm	Y/Y
AD related	BIN1	AD risk gene	Biolegend # 655602	99D	147 Sm	Y/Y
	Aβ40	Amyloid β peptide	Biolegend # 805402	11A50-B10	168 Er	Y/N
	Aβ42	Amyloid β peptide	Biolegend #851602	BA3-9.R	161 Dy	Y/N
	PHF-tau	Paired helical filament tau	Thermo #MN1020	AT8	158 Gd	Y/N
	ApoE	AD risk gene	Biolegend # 803303	D6E10	167 Er	Y/Y
PD or DLB related	TMEM230	PD risk gene	Santa Cruz # sc-398561	C20orf30 (G-2)	149 Sm	Y/Y
	DJ1	PD risk gene	Biolegend # 851502	A16125E	160 Gd	Y/Y
	LRRK2	PD risk gene	Abcam # ab170993	UDD3 30(12)	141 Pr	Y/Y

	GBA1	PD risk gene	Genzyme	8E4	164 Dy	Y/Y
	Parkin	PD risk gene	Biolegend # 808503	Prk 8	144 Nd	Y/Y
	p129-AS	Phospho-α-synuclein	Abcam # ab184674	P-syn/81A	159 Tb	Y/N
Injury & Response	Ac-Casp3	apoptosis	GeneTex# GTX86909	Poly	146 Nd	Y/N
	3-NT	oxidative stress	Sigma Millipore #05-233	1A6	165 Ho	Y/N
	EAAT1	astrocyte	Thermo # PA5-72895	poly	089 Y	Y/N
	K48	ubiquitin	Sigma Millipore # 05-1307	Apu2	174 Yb	Y/N
	LC3B	autophagy	Novus # NB100-2220	Poly	171 Yb	Y/N
	GFAP	astrocyte	Fluidigm # 3143022B	GA5	143 Nd	Y/N
Cell Energy	GATM	creatine synthesis	Novus # NBP2-00984	OTI1E3	152 Sm	Y/Y
	GAMT	creatine synthesis	Biorbyt # orb247514	poly	170 Er	Y/Y
	SLC6A8	creatinine transport	mybiosource #MBS9605963	poly	176 Lu	Y/Y

*The four negative markers were only used for gating presynapses, and were not included in subsequent clustering and analyses.

Table S3. Features (brain region, marker expression, subpopulation) that exhibited complete separation between Control vs. ADNC or Control vs. LBD.

	Control vs. ADNC			**Control vs. LBD**		
	BA9	**Hippocampus**	**Caudate**	**BA9**	**Hippocampus**	**Caudate**
A1		PHF-tau, CD47		GFAP		DAT
A2		PHF-tau, CD47	LRRK2	GFAP		
B1		PHF-tau				
B2						
C1		PHF-tau, CD47				DAT
C2		PHF-tau	LRRK2			DAT
C3		PHF-tau, CD47				DAT
C4		CD47				DAT
C5		PHF-tau				DAT
C6		PHF-tau	3NT, AS			DAT
C7		PHF-tau				DAT
C8		PHF-tau				DAT
C9		PHF-tau, CD47				DAT
C10			PHF-tau			DAT
C11						DAT

Table S4. SynTOF Panel Antibody Validation.

Antibody	**Validation** (*56*): ●=Genetic / ●=Orthogonal / ●=Independent Antibody / ●=Tagged Protein Expression ●=BioStrategies. Journal (ref) and/or website of validation report.
CD11b	● Anal Chem (*55*) ● https://www.thermofisher.com/antibody/product/CD11b-Antibody-clone-M1-70-Monoclonal/14-0112-82
MBP	● Nat Neurosci (*70*) ● Sci Rep (*71*) ●● BMC Res Notes (*72*), J Neuroimmunol (*73*)
CD56	● J Biol Chem (*74*) ●● J Neurosci Methods (*16*), Cytometry A (*17*)
SNAP25	● J Neurosci (*75*) ●● Lab Invest (*76*), J Neurosci Meth (*16*)
PSD95	● Proc Natl Acad Sci (*77*), https://www.labome.com/knockout-validated-antibodies/PSD-95-antibody-knockout-validation-NeuroMab-75-028.html#ref1, ● https://www.antibodiesinc.com/products/anti-psd-95-antibody-k28-43-75-028
Gephyrin	●● Science (*12*), https://sysy.com/product/147011.
CD47	● Nature (*78*) ● Nature (*79*), PNAS (*80*)
PrP	● Exp Eye Res (*81*) ●●●● J Neurosci Methods (*82*), Traffic (*83*), J Virol (*84*), https://www.alzforum.org/antibodies/prion-protein-3f4-0.
VGLUT	●● Am J Pathol (*35*), J Biol Chem (*85*) ● https://www.labome.com/product/Neuromab/75-066.html ●● https://www.biolegend.com/en-us/products/purified-anti-vglut1-antibody-11596?GroupID=ImportedGROUP1; https://sysy.com/product/135411.
AS	● PLoS One (*86*) ●● J Neurosci (*87*), Neurosci Lett (*88*)
Tau	● Brain Pathol (*89*) ●●● J Neurosci Res (*90*), J Neurosci (*91*), https://www.alzforum.org/antibodies/tau-total-tau-5
APP	● Neurosci (*92*) ● J Neurosci (*93*) ● J Biol Chem (*94*) ●● https://www.alzforum.org/antibodies/app-a4-22c11-1; https://www.thermofisher.com/antibody/product/APP-Amyloid-Precursor-Protein-Antibody-clone-22C11-Monoclonal/14-9749-82
GAD65	●●●● PNAS (*95*), Neuron (*96*), J Neurosci Res (*97*), J Neurosci (*98*)
Calreticulin	● https://www.thermofisher.com/antibody/product/Calreticulin-Antibody-clone-FMC-75-Monoclonal/MA1-91034 ● Oncoimmunology (*99*) ● Nat Commun (*100*)
Synapto-brevin2	●●● J Biol Chem (*101*), Science (*102*), https://sysy.com/product/104211
VMAT2	● Front Neurosci (*103*) ● https://www.abcam.com/vmat2-antibody-ab191121.html?productWallTab=ShowAll.
SERT	● https://www.sigmaaldrich.com/US/en/product/SIGMA/SAB2500950
DAT	● Lab Invest (*76*) ● Nat Commun (*104*) ●●●● Am J Pathol (*35*), Lab Invest (*76*), J Neurosci Methods (*16*), Cell (*105*)
BIN1	● https://www.origene.com/catalog/antibodies/primary-antibodies/ta319582/bin1-mouse-monoclonal-antibody-clone-id-99d
Aβ40	● PNAS (*106*) ●● PNAS (*106*), Brain Pathol (*107*)
Aβ42	● PNAS (*106*)

	● J Neurosci Methods (*16*)		
PHF-tau	● Acta Neuropathol (*108*) ●●●●PNAS (*109*), PNAS (*110*), J Neurosci (*111*), Angew Chem Int Ed Engl (*112*)		
ApoE	● PLoS Genet (*113*) ● Am J Pathol (*114*) ● Nat Commun (*115*)		
TMEM230	● J Alzheimers Dis (*116*) ●● Nat Neurosci (*70*), https://www.scbt.com/p/tmem230-antibody-g-2		
DJ-1	● Science (*116*) ● https://www.biolegend.com/en-us/products/hrp-anti-dj-1-park7-antibody-15812?GroupID=GROUP792		
LRRK2	●● Biochem J (*117*), https://www.abcam.com/lrrk2-antibody-udd3-3012-bsa-and-azide-free-ab170993.html?productWallTab=ShowAll, ● Biochem J (*117*)		
GBA1	● Nat Commun, (*118*)		
Parkin	● J Biol Chem (*119*) ●● J Biol Chem, (*119*), https://www.biolegend.com/en-us/search-results/purified-anti-parkin-antibody-11508		
p129-AS	● Commun Biol (*120*)		
Ac-Casp3	● Mol Med Rep (*121*) ● https://www.genetex.com/Product/Detail/Caspase-3-cleaved-Asp175-antibody/GTX86909#datasheet.		
3NT	● J Clin Invest (*122*) ●● Am J Pathol (*123*), Mol Brain (*124*)		
EAAT1	● https://www.thermofisher.com/antibody/product/GLAST-Antibody-Polyclonal/PA5-72895.		
K48	● Cell (*125*) ●● Sci Rep (*126*), https://www.sigmaaldrich.com/US/en/product/mm/051307		
LC3B	● https://www.novusbio.com/products/lc3b-antibody_nb100-2220 ● https://www.novusbio.com/products/lc3b-antibody_nb100-2220		
GFAP	●● ASN Neuro (*127*), Exp Cell Res (*128*) ● https://www.thermofisher.com/antibody/product/GFAP-Antibody-clone-GA5-Monoclonal/14-9892-82.		
GATM	● Western blot ● Brain Res (*129*)	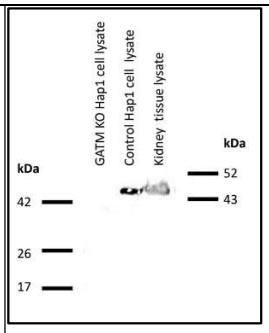	**GATM antibody validation by Western blot.** GATM knockout (KO) cells were derived by CRISPR/Cas-9 deletion of 2bp in exon 5 in Hap1 cells (genomic location Chr15:45366402; Horizon Discovery Cat# HZGHC007887c010). Parental Hap1 cells (Horizon Discovery Cat# C631) and wild type C57Bl/6 mouse kidney were used as controls. 20ug protein/lysate was separated by gel electrophoresis, transferred to membrane, blocked, and probed with primary antibody to GATM (1:250). *Source: Montine laboratory, unpublished result,.*
GAMT	● Brain Res (*129*)		
SLC6A8	● J Inherit Metab Dis (*130*) ● https://www.mybiosource.com/polyclonal-human-mouse-rat-antibody/slc6a8/9605963		

REFERENCES AND NOTES

1. S. W. Scheff, D. A. Price, Synaptic pathology in Alzheimer's disease: A review of ultrastructural studies. *Neurobiol. Aging* **24**, 1029–1046 (2003).

2. R. D. Terry, E. Masliah, D. P. Salmon, N. Butters, R. DeTeresa, R. Hill, L. A. Hansen, R. Katzman, Physical basis of cognitive alterations in Alzheimer's disease: Synapse loss is the major correlate of cognitive impairment. *Ann. Neurol.* **30**, 572–580 (1991).

3. E. Masliah, R. D. Terry, M. Alford, R. DeTeresa, L. A. Hansen, Cortical and subcortical patterns of synaptophysinlike immunoreactivity in Alzheimer's disease. *Am. J. Pathol.* **138**, 235–246 (1991).

4. B. T. Hyman, G. W. Van Hoesen, L. J. Kromer, A. R. Damasio, Perforant pathway changes and the memory impairment of Alzheimer's disease. *Ann. Neurol.* **20**, 472–481 (1986).

5. S. T. DeKosky, S. W. Scheff, Synapse loss in frontal cortex biopsies in Alzheimer's disease: Correlation with cognitive severity. *Ann. Neurol.* **27**, 457–464 (1990).

6. K. H. Gylys, T. Bilousova, Flow cytometry analysis and quantitative characterization of tau in synaptosomes from Alzheimer's disease brains. *Methods Mol. Biol.* **1523**, 273–284 (2017).

7. B. C. Yoo, N. Cairns, M. Fountoulakis, G. Lubec, Synaptosomal proteins, beta-soluble N-ethylmaleimide-sensitive factor attachment protein (beta-SNAP), gamma-SNAP and synaptotagmin I in brain of patients with Down syndrome and Alzheimer's disease. *Dement. Geriatr. Cogn. Disord.* **12**, 219–225 (2001).

8. T. S. Wijasa, M. Sylvester, N. Brocke-Ahmadinejad, S. Schwartz, F. Santarelli, V. Gieselmann, T. Klockgether, F. Brosseron, M. T. Heneka, Quantitative proteomics of synaptosome S-nitrosylation in Alzheimer's disease. *J. Neurochem.* **152**, 710–726 (2020).

9. B. G. Perez-Nievas, T. D. Stein, H. C. Tai, O. Dols-Icardo, T. C. Scotton, I. Barroeta-Espar, L. Fernandez-Carballo, E. L. de Munain, J. Perez, M. Marquie, A. Serrano-Pozo, M. P. Frosch, V. Lowe, J. E. Parisi, R. C. Petersen, M. D. Ikonomovic, O. L. López, W. Klunk, B. T. Hyman, T.

Gómez-Isla, Dissecting phenotypic traits linked to human resilience to Alzheimer's pathology. *Brain* **136**, 2510–2526 (2013).

10. F. Koopmans, P. van Nierop, M. Andres-Alonso, A. Byrnes, T. Cijsouw, M. P. Coba, L. N. Cornelisse, R. J. Farrell, H. L. Goldschmidt, D. P. Howrigan, N. K. Hussain, C. Imig, A. P. H. de Jong, H. Jung, M. Kohansalnodehi, B. Kramarz, N. Lipstein, R. C. Lovering, H. M. Gillavry, V. Mariano, H. Mi, M. Ninov, D. Osumi-Sutherland, R. Pielot, K.-H. Smalla, H. Tang, K. Tashman, R. F. G. Toonen, C. Verpelli, R. Reig-Viader, K. Watanabe, J. van Weering, T. Achsel, G. Ashrafi, N. Asi, T. C. Brown, P. De Camilli, M. Feuermann, R. E. Foulger, P. Gaudet, A. Joglekar, A. Kanellopoulos, R. Malenka, R. A. Nicoll, C. Pulido, J. de Juan-Sanz, M. Sheng, T. C. Südhof, H. U. Tilgner, C. Bagni, À. Bayés, T. Biederer, N. Brose, J. J. E. Chua, D. C. Dieterich, E. D. Gundelfinger, C. Hoogenraad, R. L. Huganir, R. Jahn, P. S. Kaeser, E. Kim, M. R. Kreutz, P. S. McPherson, B. M. Neale, V. O'Conner, D. Posthuma, T. A. Ryan, C. Sala, G. Feng, S. E. Hyman, P. D. Thomas, A. B. Smit, M. Verhage, SynGO: An evidence-based, expert-curated knowledge base for the synapse. *Neuron* **103**, 217–234.e4 (2019).

11. E. C. B. Johnson, E. B. Dammer, D. M. Duong, L. Ping, M. Zhou, L. Yin, L. A. Higginbotham, A. Guajardo, B. White, J. C. Troncoso, M. Thambisetty, T. J. Montine, E. B. Lee, J. Q. Trojanowski, T. G. Beach, E. M. Reiman, V. Haroutunian, M. Wang, E. Schadt, B. Zhang, D. W. Dickson, N. Ertekin-Taner, T. E. Golde, V. A. Petyuk, P. L. de Jager, D. A. Bennett, T. S. Wingo, S. Rangaraju, I. Hajjar, J. M. Shulman, J. J. Lah, A. I. Levey, N. T. Seyfried, Large-scale proteomic analysis of Alzheimer's disease brain and cerebrospinal fluid reveals early changes in energy metabolism associated with microglia and astrocyte activation. *Nat. Med.* **26**, 769–780 (2020).

12. A. P. Wingo, E. B. Dammer, M. S. Breen, B. A. Logsdon, D. M. Duong, J. C. Troncosco, M. Thambisetty, T. G. Beach, G. E. Serrano, E. M. Reiman, R. J. Caselli, J. J. Lah, N. T. Seyfried, A. I. Levey, T. S. Wingo, Large-scale proteomic analysis of human brain identifies proteins associated with cognitive trajectory in advanced age. *Nat. Commun.* **10**, 1619 (2019).

13. C. M. Henstridge, R. J. Jackson, J. S. M. Kim, A. G. Herrmann, A. K. Wright, S. E. Harris, M. E. Bastin, J. M. Starr, J. Wardlaw, T. H. Gillingwater, C. Smith, C. A. McKenzie, S. R. Cox, I. J. Deary, T. L. Spires-Jones, Post-mortem brain analyses of the Lothian Birth Cohort 1936: Extending

lifetime cognitive and brain phenotyping to the level of the synapse. *Acta Neuropathol. Commun.* **3**, 53 (2015).

14. M. Colom-Cadena, J. Pegueroles, A. G. Herrmann, C. M. Henstridge, L. Muñoz, M. Querol-Vilaseca, C. S. Martín-Paniello, J. Luque-Cabecerans, J. Clarimon, O. Belbin, R. Núñez-Llaves, R. Blesa, C. Smith, C. A. McKenzie, M. P. Frosch, A. Roe, J. Fortea, J. Andilla, P. Loza-Alvarez, E. Gelpi, B. T. Hyman, T. L. Spires-Jones, A. Lleó, Synaptic phosphorylated α-synuclein in dementia with Lewy bodies. *Brain* **140**, 3204–3214 (2017).

15. H. C. Tai, B. Y. Wang, A. Serrano¿Pozo, M. P. Frosch, T. L. Spires-Jones, B. T. Hyman, Frequent and symmetric deposition of misfolded tau oligomers within presynaptic and postsynaptic terminals in Alzheimer¿s disease. *Acta Neuropathol. Commun.* **2**, 146 (2014).

16. C. R. Gajera, R. Fernandez, N. Postupna, K. S. Montine, E. J. Fox, D. Tebaykin, M. Angelo, S. C. Bendall, C. D. Keene, T. J. Montine, Mass synaptometry: High-dimensional multi parametric assay for single synapses. *J. Neurosci. Methods* **312**, 73–83 (2019).

17. C. R. Gajera, R. Fernandez, K. S. Montine, E. J. Fox, D. Mrdjen, N. O. Postupna, C. D. Keene, S. C. Bendall, T. J. Montine, Mass-tag barcoding for multiplexed analysis of human synaptosomes and other anuclear events. *Cytometry A* **99**, 939–945 (2021).

18. B. T. Hyman, C. H. Phelps, T. G. Beach, E. H. Bigio, N. J. Cairns, M. C. Carrillo, D. W. Dickson, C. Duyckaerts, M. P. Frosch, E. Masliah, S. S. Mirra, P. T. Nelson, J. A. Schneider, D. R. Thal, B. Thies, J. Q. Trojanowski, H. V. Vinters, T. J. Montine, National Institute on Aging-Alzheimer's Association guidelines for the neuropathologic assessment of Alzheimer's disease. *Alzheimers Dement.* **8**, 1–13 (2012).

19. T. J. Montine, C. H. Phelps, T. G. Beach, E. H. Bigio, N. J. Cairns, D. W. Dickson, C. Duyckaerts, M. P. Frosch, E. Masliah, S. S. Mirra, P. T. Nelson, J. A. Schneider, D. R. Thal, J. Q. Trojanowski, H. V. Vinters, B. T. Hyman; National Institute on Aging.; Alzheimer’s Association., National Institute on Aging-Alzheimer's Association guidelines for the neuropathologic assessment of Alzheimer's disease: A practical approach. *Acta Neuropathol.* **123**, 1–11 (2012).

20. T. J. Montine, S. A. Bukhari, L. R. White, Cognitive impairment in older adults and therapeutic strategies. *Pharmacol. Rev.* **73**, 152–162 (2021).

21. P. Somogyi, G. Tamás, R. Lujan, E. H. Buhl, Salient features of synaptic organisation in the cerebral cortex. *Brain Res. Brain Res. Rev.* **26**, 113–135 (1998).

22. J. P. Bolam, E. K. Pissadaki, Living on the edge with too many mouths to feed: Why dopamine neurons die. *Mov. Disord.* **27**, 1478–1483 (2012).

23. J. F. Smiley, P. S. Goldman-Rakic, Heterogeneous targets of dopamine synapses in monkey prefrontal cortex demonstrated by serial section electron microscopy: A laminar analysis using the silver-enhanced diaminobenzidine sulfide (SEDS) immunolabeling technique. *Cereb. Cortex* **3**, 223–238 (1993).

24. C. J. Lacey, J. Boyes, O. Gerlach, L. Chen, P. J. Magill, J. P. Bolam, GABA(B) receptors at glutamatergic synapses in the rat striatum. *Neuroscience* **136**, 1083–1095 (2005).

25. V. J. Roberts, S. L. Barth, H. Meunier, W. Vale, Hybridization histochemical and immunohistochemical localization of inhibin/activin subunits and messenger ribonucleic acids in the rat brain. *J. Comp. Neurol.* **364**, 473–493 (1996).

26. G. W. Miller, J. D. Erickson, J. T. Perez, S. N. Penland, D. C. Mash, D. B. Rye, A. I. Levey, Immunochemical analysis of vesicular monoamine transporter (VMAT2) protein in Parkinson's disease. *Exp. Neurol.* **156**, 138–148 (1999).

27. J. Booij, G. Tissingh, G. J. Boer, J. D. Speelman, J. C. Stoof, A. G. Janssen, E. C. Wolters, E. A. van Royen, [123I]FP-CIT SPECT shows a pronounced decline of striatal dopamine transporter labelling in early and advanced Parkinson's disease. *J. Neurol. Neurosurg. Psychiatry* **62**, 133–140 (1997).

28. H. Sasaguri, P. Nilsson, S. Hashimoto, K. Nagata, T. Saito, B. de Strooper, J. Hardy, R. Vassar, B. Winblad, T. C. Saido, APP mouse models for Alzheimer's disease preclinical studies. *EMBO J.* **36**, 2473–2487 (2017).

29. L. Mucke, D. J. Selkoe, Neurotoxicity of amyloid β-protein: Synaptic and network dysfunction. *Cold Spring Harb. Perspect. Med.* **2**, a006338 (2012).

30. N. Aghaeepour, E. F. Simonds, D. J. H. F. Knapp, R. V. Bruggner, K. Sachs, A. Culos, P. F. Gherardini, N. Samusik, G. K. Fragiadakis, S. C. Bendall, B. Gaudilliere, M. S. Angst, C. J. Eaves, W. A. Weiss, W. J. Fantl, G. P. Nolan, GateFinder: Projection-based gating strategy optimization for flow and mass cytometry. *Bioinformatics* **34**, 4131–4133 (2018).

31. I. G. McKeith, B. F. Boeve, D. W. Dickson, G. Halliday, J. P. Taylor, D. Weintraub, D. Aarsland, J. Galvin, J. Attems, C. G. Ballard, A. Bayston, T. G. Beach, F. Blanc, N. Bohnen, L. Bonanni, J. Bras, P. Brundin, D. Burn, A. Chen-Plotkin, J. E. Duda, O. el-Agnaf, H. Feldman, T. J. Ferman, D. ffytche, H. Fujishiro, D. Galasko, J. G. Goldman, S. N. Gomperts, N. R. Graff-Radford, L. S. Honig, A. Iranzo, K. Kantarci, D. Kaufer, W. Kukull, V. M. Y. Lee, J. B. Leverenz, S. Lewis, C. Lippa, A. Lunde, M. Masellis, E. Masliah, P. McLean, B. Mollenhauer, T. J. Montine, E. Moreno, E. Mori, M. Murray, J. T. O'Brien, S. Orimo, R. B. Postuma, S. Ramaswamy, O. A. Ross, D. P. Salmon, A. Singleton, A. Taylor, A. Thomas, P. Tiraboschi, J. B. Toledo, J. Q. Trojanowski, D. Tsuang, Z. Walker, M. Yamada, K. Kosaka, Diagnosis and management of dementia with Lewy bodies: Fourth consensus report of the DLB Consortium. *Neurology* **89**, 88–100 (2017).

32. M. Ballmaier, J. T. O'Brien, E. J. Burton, P. M. Thompson, D. E. Rex, K. L. Narr, I. G. McKeith, H. DeLuca, A. W. Toga, Comparing gray matter loss profiles between dementia with Lewy bodies and Alzheimer's disease using cortical pattern matching: Diagnosis and gender effects. *NeuroImage* **23**, 325–335 (2004).

33. L. Keren, M. Bosse, S. Thompson, T. Risom, K. Vijayaragavan, E. M. Caffrey, D. Marquez, R. Angoshtari, N. F. Greenwald, H. Fienberg, J. Wang, N. Kambham, D. Kirkwood, G. Nolan, T. J. Montine, S. J. Galli, R. West, S. C. Bendall, M. Angelo, MIBI-TOF: A multiplexed imaging platform relates cellular phenotypes and tissue structure. *Sci. Adv.* **5**, eaax5851 (2019).

34. V. Rangaraju, N. Calloway, T. A. Ryan, Activity-driven local ATP synthesis is required for synaptic function. *Cell* **156**, 825–835 (2014).

35. N. Postupna, C. S. Latimer, E. B. Larson, E. Sherfield, J. Paladin, C. A. Shively, M. J. Jorgensen, R. N. Andrews, J. R. Kaplan, P. K. Crane, K. S. Montine, S. Craft, C. D. Keene, T. J. Montine, Human striatal dopaminergic and regional serotonergic synaptic degeneration with lewy body disease and inheritance of APOE ε4. *Am. J. Pathol.* **187**, 884–895 (2017).

36. M. Gratuze, D. M. Holtzman, Targeting pre-synaptic tau accumulation: A new strategy to counteract tau-mediated synaptic loss and memory deficits. *Neuron* **109**, 741–743 (2021).

37. À. Bayés, M. O. Collins, R. Reig-Viader, G. Gou, D. Goulding, A. Izquierdo, J. S. Choudhary, R. D. Emes, S. G. N. Grant, Evolution of complexity in the zebrafish synapse proteome. *Nat. Commun.* **8**, 14613 (2017).

38. B. C. Carlyle *et al.*, Multiplexed fractionated proteomics reveals synaptic factors associated with cognitive resilience in Alzheimer's disease. bioRxiv 2020.07.31.230680 [**Preprint**]. 1 August 2020. https://doi.org/10.1101/2020.07.31.230680.

39. J. Choi, M. C. Sullards, J. A. Olzmann, H. D. Rees, S. T. Weintraub, D. E. Bostwick, M. Gearing, A. I. Levey, L. S. Chin, L. Li, Oxidative damage of DJ-1 is linked to sporadic Parkinson and Alzheimer diseases. *J. Biol. Chem.* **281**, 10816–10824 (2006).

40. K. Solti, W. L. Kuan, B. Fórizs, G. Kustos, J. Mihály, Z. Varga, B. Herberth, É. Moravcsik, R. Kiss, M. Kárpáti, A. Mikes, Y. Zhao, T. Imre, J. C. Rochet, F. Aigbirhio, C. H. Williams-Gray, R. A. Barker, G. Tóth, DJ-1 can form β-sheet structured aggregates that co-localize with pathological amyloid deposits. *Neurobiol. Dis.* **134**, 104629 (2020).

41. D. J. Moore, L. Zhang, J. Troncoso, M. K. Lee, N. Hattori, Y. Mizuno, T. M. Dawson, V. L. Dawson, Association of DJ-1 and parkin mediated by pathogenic DJ-1 mutations and oxidative stress. *Hum. Mol. Genet.* **14**, 71–84 (2005).

42. P. Heutink, PINK-1 and DJ-1—New genes for autosomal recessive Parkinson's disease. *J. Neural Transm. Suppl.* **2006**, 215–219 (2006).

43. T. J. Montine, K. S. Montine, W. McMahan, W. R. Markesbery, J. F. Quinn, J. D. Morrow, F2-isoprostanes in Alzheimer and other neurodegenerative diseases. *Antioxid. Redox Signal.* **7**, 269–275 (2005).

44. H. Ohnishi, Y. Kaneko, H. Okazawa, M. Miyashita, R. Sato, A. Hayashi, K. Tada, S. Nagata, M. Takahashi, T. Matozaki, Differential localization of Src homology 2 domain-containing protein tyrosine phosphatase substrate-1 and CD47 and its molecular mechanisms in cultured hippocampal neurons. *J. Neurosci.* **25**, 2702–2711 (2005).

45. A. B. Toth, A. Terauchi, L. Y. Zhang, E. M. Johnson-Venkatesh, D. J. Larsen, M. A. Sutton, H. Umemori, Synapse maturation by activity-dependent ectodomain shedding of SIRPα. *Nat. Neurosci.* **16**, 1417–1425 (2013).

46. T. W. Miller, J. S. Isenberg, H. B. Shih, Y. Wang, D. D. Roberts, Amyloid-β inhibits No-cGMP signaling in a CD36- and CD47-dependent manner. *PLOS ONE* **5**, e15686 (2010).

47. M. H. Han, D. H. Lundgren, S. Jaiswal, M. Chao, K. L. Graham, C. S. Garris, R. C. Axtell, P. P. Ho, C. B. Lock, J. I. Woodard, S. E. Brownell, M. Zoudilova, J. F. V. Hunt, S. E. Baranzini, E. C. Butcher, C. S. Raine, R. A. Sobel, D. K. Han, I. Weissman, L. Steinman, Janus-like opposing roles of CD47 in autoimmune brain inflammation in humans and mice. *J. Exp. Med.* **209**, 1325–1334 (2012).

48. E. K. Lehrman, D. K. Wilton, E. Y. Litvina, C. A. Welsh, S. T. Chang, A. Frouin, A. J. Walker, M. D. Heller, H. Umemori, C. Chen, B. Stevens, CD47 protects synapses from excess microglia-mediated pruning during development. *Neuron* **100**, 120–134.e6 (2018).

49. T. Bartels, S. De Schepper, S. Hong, Microglia modulate neurodegeneration in Alzheimer's and Parkinson's diseases. *Science* **370**, 66–69 (2020).

50. M. P. Chao, C. H. Takimoto, D. D. Feng, K. M. Kenna, P. Gip, J. Liu, J.-P. Volkmer, I. L. Weissman, R. Majeti, Therapeutic targeting of the macrophage immune checkpoint CD47 in myeloid malignancies. *Front. Oncol.* **9**, 1380 (2020).

51. J. D. Ulrich, T. K. Ulland, T. E. Mahan, S. Nyström, K. P. Nilsson, W. M. Song, Y. Zhou, M. Reinartz, S. Choi, H. Jiang, F. R. Stewart, E. Anderson, Y. Wang, M. Colonna, D. M. Holtzman, ApoE facilitates the microglial response to amyloid plaque pathology. *J. Exp. Med.* **215**, 1047–1058 (2018).

52. Y. Shi, K. Yamada, S. A. Liddelow, S. T. Smith, L. Zhao, W. Luo, R. M. Tsai, S. Spina, L. T. Grinberg, J. C. Rojas, G. Gallardo, K. Wang, J. Roh, G. Robinson, M. B. Finn, H. Jiang, P. M. Sullivan, C. Baufeld, M. W. Wood, C. Sutphen, L. M. Cue, C. Xiong, J. L. Del-Aguila, J. C. Morris, C. Cruchaga; Alzheimer's Disease Neuroimaging Initiative, A. M. Fagan, B. L. Miller, A. L. Boxer, W. W. Seeley, O. Butovsky, B. A. Barres, S. M. Paul, D. M. Holtzman, ApoE4 markedly exacerbates tau-mediated neurodegeneration in a mouse model of tauopathy. *Nature* **549**, 523–527 (2017).

53. T.-P. V. Huynh, F. Liao, C. M. Francis, G. O. Robinson, J. R. Serrano, H. Jiang, J. Roh, M. B. Finn, P. M. Sullivan, T. J. Esparza, F. R. Stewart, T. E. Mahan, J. D. Ulrich, T. Cole, D. M. Holtzman, Age-dependent effects of apoE reduction using antisense oligonucleotides in a model of β-amyloidosis. *Neuron* **96**, 1013–1023.e4 (2017).

54. G. M. McKhann, D. S. Knopman, H. Chertkow, B. T. Hyman, C. R. Jack Jr, C. H. Kawas, W. E. Klunk, W. J. Koroshetz, J. J. Manly, R. Mayeux, R. C. Mohs, J. C. Morris, M. N. Rossor, P. Scheltens, M. C. Carrillo, B. Thies, S. Weintraub, C. H. Phelps, The diagnosis of dementia due to Alzheimer's disease: Recommendations from the National Institute on Aging-Alzheimer's Association workgroups on diagnostic guidelines for Alzheimer's disease. *Alzheimers Dement.* **7**, 263–269 (2011).

55. D. R. Bandura, V. I. Baranov, O. I. Ornatsky, A. Antonov, R. Kinach, X. Lou, S. Pavlov, S. Vorobiev, J. E. Dick, S. D. Tanner, Mass cytometry: Technique for real time single cell multitarget immunoassay based on inductively coupled plasma time-of-flight mass spectrometry. *Anal. Chem.* **81**, 6813–6822 (2009).

56. M. Uhlen, A. Bandrowski, S. Carr, A. Edwards, J. Ellenberg, E. Lundberg, D. L. Rimm, H. Rodriguez, T. Hiltke, M. Snyder, T. Yamamoto, A proposal for validation of antibodies. *Nat. Methods* **13**, 823–827 (2016).

57. L. Holcomb, M. N. Gordon, E. McGowan, X. Yu, S. Benkovic, P. Jantzen, K. Wright, I. Saad, R. Mueller, D. Morgan, S. Sanders, C. Zehr, K. O'Campo, J. Hardy, C. M. Prada, C. Eckman, S. Younkin, K. Hsiao, K. Duff, Accelerated Alzheimer-type phenotype in transgenic mice carrying both mutant amyloid precursor protein and presenilin 1 transgenes. *Nat. Med.* **4**, 97–100 (1998).

58. N. Stanley, I. A. Stelzer, A. S. Tsai, R. Fallahzadeh, E. Ganio, M. Becker, T. Phongpreecha, H. Nassar, S. Ghaemi, I. Maric, A. Culos, A. L. Chang, M. Xenochristou, X. Han, C. Espinosa, K. Rumer, L. Peterson, F. Verdonk, D. Gaudilliere, E. Tsai, D. Feyaerts, J. Einhaus, K. Ando, R. J. Wong, G. Obermoser, G. M. Shaw, D. K. Stevenson, M. S. Angst, B. Gaudilliere, N. Aghaeepour, VoPo leverages cellular heterogeneity for predictive modeling of single-cell data. *Nat. Commun.* **11**, 3738 (2020).

59. S. Van Gassen, B. Callebaut, M. J. Van Helden, B. N. Lambrecht, P. Demeester, T. Dhaene, Y. Saeys, FlowSOM: Using self-organizing maps for visualization and interpretation of cytometry data. *Cytometry A* **87**, 636–645 (2015).

60. L. M. Weber, M. D. Robinson, Comparison of clustering methods for high-dimensional single-cell flow and mass cytometry data. *Cytometry A* **89**, 1084–1096 (2016).

61. X. Liu, W. Song, B. Y. Wong, T. Zhang, S. Yu, G. N. Lin, X. Ding, A comparison framework and guideline of clustering methods for mass cytometry data. *Genome Biol.* **20**, 297 (2019).

62. X. Guo, L. Gao, X. Liu, J. Yin, Improved deep embedded clustering with local structure preservation, in *Proceedings of the Twenty-Sixth International Joint Conference on Artificial Intelligence* (IJCAI, 2017), pp. 1753–1759.

63. K. Hornik, A CLUE for CLUster ensembles. *J. Stat. Softw.* **14**, 1–25 (2005).

64. K. H. Gylys, J. A. Fein, G. M. Cole, Quantitative characterization of crude synaptosomal fraction (P-2) components by flow cytometry. *J. Neurosci. Res.* **61**, 186–192 (2000).

65. K. H. Gylys, J. A. Fein, F. Yang, D. J. Wiley, C. A. Miller, G. M. Cole, Synaptic changes in Alzheimer's disease: Increased amyloid-beta and gliosis in surviving terminals is accompanied by decreased PSD-95 fluorescence. *Am. J. Pathol.* **165**, 1809–1817 (2004).

66. A. Culos, A. S. Tsai, N. Stanley, M. Becker, M. S. Ghaemi, D. R. McIlwain, R. Fallahzadeh, A. Tanada, H. Nassar, C. Espinosa, M. Xenochristou, E. Ganio, L. Peterson, X. Han, I. A. Stelzer, K. Ando, D. Gaudilliere, T. Phongpreecha, I. Marić, A. L. Chang, G. M. Shaw, D. K. Stevenson, S. Bendall, K. L. Davis, W. Fantl, G. P. Nolan, T. Hastie, R. Tibshirani, M. S. Angst, B. Gaudilliere, N. Aghaeepour, Integration of mechanistic immunological knowledge into a machine learning pipeline improves predictions. *Nat. Mach. Intell.* **2**, 619–628 (2020).

67. T. Phongpreecha, R. Fernandez, D. Mrdjen, A. Culos, C. R. Gajera, A. M. Wawro, N. Stanley, B. Gaudilliere, K. L. Poston, N. Aghaeepour, T. J. Montine, Single-cell peripheral immunoprofiling of Alzheimer's and Parkinson's diseases. *Sci. Adv.* **6**, eabd5575 (2020).

68. M. M. B. Bosse, S. C. Bendall, M. R. Angelo, MIBI staining: Human BioMolecular Atlas Program (HuBMAP) Method Development Community. protocols.io. 2021 (dx.doi.org/10.17504/protocols.io.bt9tnr6n).

69. M. M. B. Bosse, S. C. Camacho, S. C. Bendall, M. R. Angelo, MIBI and IHC solutions: Human BioMolecular Atlas Program (HuBMAP) Method Development Community. protocols.io.2021 (dx.doi.org/10.17504/protocols.io.bhmej43e).

70. M. Traka, J. R. Podojil, D. P. McCarthy, S. D. Miller, B. Popko, Oligodendrocyte death results in immune-mediated CNS demyelination. *Nat. Neurosci.* **19**, 65–74 (2016).

71. T. Barron, J. Saifetiarova, M. A. Bhat, J. H. Kim, Myelination of Purkinje axons is critical for resilient synaptic transmission in the deep cerebellar nucleus. *Sci. Rep.* **8**, 1022 (2018).

72. J. M. Boggs, L. Homchaudhuri, G. Ranagaraj, Y. Liu, G. S. T. Smith, G. Harauz, Interaction of myelin basic protein with cytoskeletal and signaling proteins in cultured primary oligodendrocytes and N19 oligodendroglial cells. *BMC Res. Notes* **7**, 387 (2014).

73. R. R. Voskuhl, T. M. Pribyl, K. Kampf, V. Handley, H. B. Liu, J. M. Feng, C. W. Campagnoni, S. S. Soldan, A. Messing, A. T. Campagnoni, Experimental autoimmune encephalomyelitis relapses are reduced in heterozygous golli MBP knockout mice. *J. Neuroimmunol.* **139**, 44–50 (2003).

74. E. M. Treutlein, K. Kern, A. Weigert, N. Tarighi, C. D. Schuh, R. M. Nüsing, Y. Schreiber, N. Ferreirós, B. Brüne, G. Geisslinger, S. Pierre, K. Scholich, The prostaglandin E2 receptor EP3 controls CC-chemokine ligand 2-mediated neuropathic pain induced by mechanical nerve damage. *J. Biol. Chem.* **293**, 9685–9695 (2018).

75. L. C. Tafoya, M. Mameli, T. Miyashita, J. F. Guzowski, C. F. Valenzuela, M. C. Wilson, Expression and function of SNAP-25 as a universal SNARE component in GABAergic neurons. *J. Neurosci.* **26**, 7826–7838 (2006).

76. N. O. Postupna, C. D. Keene, C. Latimer, E. E. Sherfield, R. D. van Gelder, J. G. Ojemann, T. J. Montine, M. Darvas, Flow cytometry analysis of synaptosomes from post-mortem human brain reveals changes specific to Lewy body and Alzheimer's disease. *Lab. Investig.* **94**, 1161–1172 (2014).

77. S. Won, S. Incontro, R. A. Nicoll, K. W. Roche, PSD-95 stabilizes NMDA receptors by inducing the degradation of STEP61. *Proc. Natl. Acad. Sci. U.S.A.* **113**, E4736–E4744 (2016).

78. S. R. Gordon, R. L. Maute, B. W. Dulken, G. Hutter, B. M. George, M. N. McCracken, R. Gupta, J. M. Tsai, R. Sinha, D. Corey, A. M. Ring, A. J. Connolly, I. L. Weissman, PD-1 expression by tumour-associated macrophages inhibits phagocytosis and tumour immunity. *Nature* **545**, 495–499 (2017).

79. Y. Kojima, J. P. Volkmer, K. McKenna, M. Civelek, A. J. Lusis, C. L. Miller, D. Direnzo, V. Nanda, J. Ye, A. J. Connolly, E. E. Schadt, T. Quertermous, P. Betancur, L. Maegdefessel, L. P. Matic, U. Hedin, I. L. Weissman, N. J. Leeper, CD47-blocking antibodies restore phagocytosis and prevent atherosclerosis. *Nature* **536**, 86–90 (2016).

80. S. B. Willingham, J. P. Volkmer, A. J. Gentles, D. Sahoo, P. Dalerba, S. S. Mitra, J. Wang, H. Contreras-Trujillo, R. Martin, J. D. Cohen, P. Lovelace, F. A. Scheeren, M. P. Chao, K. Weiskopf, C. Tang, A. K. Volkmer, T. J. Naik, T. A. Storm, A. R. Mosley, B. Edris, S. M. Schmid, C. K. Sun, M. S. Chua, O. Murillo, P. Rajendran, A. C. Cha, R. K. Chin, D. Kim, M. Adorno, T. Raveh, D. Tseng, S. Jaiswal, P. O. Enger, G. K. Steinberg, G. Li, S. K. So, R. Majeti, G. R. Harsh, M. van de Rijn, N. N. H. Teng, J. B. Sunwoo, A. A. Alizadeh, M. F. Clarke, I. L. Weissman, The CD47-signal

regulatory protein alpha (SIRPa) interaction is a therapeutic target for human solid tumors. *Proc. Natl. Acad. Sci. U.S.A.* **109**, 6662–6667 (2012).

81. A. Ashok, S. Karmakar, R. Chandel, R. Ravikumar, S. Dalal, Q. Kong, N. Singh, Prion protein modulates iron transport in the anterior segment: Implications for ocular iron homeostasis and prion transmission. *Exp. Eye Res.* **175**, 1–13 (2018).

82. C. Lund, C. M. Olsen, H. Tveit, M. A. Tranulis, Characterization of the prion protein 3F4 epitope and its use as a molecular tag. *J. Neurosci. Methods* **165**, 183–190 (2007).

83. R. J. Kascsak, R. Rubenstein, P. A. Merz, M. Tonna-DeMasi, R. Fersko, R. I. Carp, H. M. Wisniewski, H. Diringer, Mouse polyclonal and monoclonal antibody to scrapie-associated fibril proteins. *J. Virol.* **61**, 3688–3693 (1987).

84. S. Gilch, M. Nunziante, A. Ertmer, F. Wopfner, L. Laszlo, H. M. Schätzl, Recognition of lumenal prion protein aggregates by post-ER quality control mechanisms is mediated by the preoctarepeat region of PrP. *Traffic* **5**, 300–313 (2004).

85. S. V. Yelamanchili, G. Pendyala, I. Brunk, M. Darna, U. Albrecht, G. Ahnert-Hilger, Differential sorting of the vesicular glutamate transporter 1 into a defined vesicular pool is regulated by light signaling involving the clock gene Period2. *J. Biol. Chem.* **281**, 15671–15679 (2006).

86. H. Dimant, L. Zhu, L. N. Kibuuka, Z. Fan, B. T. Hyman, P. J. McLean, Direct visualization of CHIP-mediated degradation of alpha-synuclein in vivo: Implications for PD therapeutics. *PLOS ONE* **9**, e92098 (2014).

87. M. E. Larson, M. A. Sherman, S. Greimel, M. Kuskowski, J. A. Schneider, D. A. Bennett, S. E. Lesne, Soluble α-synuclein is a novel modulator of Alzheimer's disease pathophysiology. *J. Neurosci.* **32**, 10253–10266 (2012).

88. R. Jakes, R. A. Crowther, V. M. Y. Lee, J. Q. Trojanowski, T. Iwatsubo, M. Goedert, Epitope mapping of LB509, a monoclonal antibody directed against human alpha-synuclein. *Neurosci. Lett.* **269**, 13–16 (1999).

89. M. Fernández-Nogales, M. Santos-Galindo, J. Merchán-Rubira, J. J. M. Hoozemans, A. Rábano, I. Ferrer, J. Avila, F. Hernández, J. J. Lucas, Tau-positive nuclear indentations in P301S tauopathy mice. *Brain Pathol.* **27**, 314–322 (2017).

90. M. Demars, Y. S. Hu, A. Gadadhar, O. Lazarov, Impaired neurogenesis is an early event in the etiology of familial Alzheimer's disease in transgenic mice. *J. Neurosci. Res.* **88**, 2103–2117 (2010).

91. D. M. Wilcock, M. R. Lewis, W. E. van Nostrand, J. Davis, M. L. Previti, N. Gharkholonarehe, M. P. Vitek, C. A. Colton, Progression of amyloid pathology to Alzheimer's disease pathology in an amyloid precursor protein transgenic mouse model by removal of nitric oxide synthase 2. *J. Neurosci.* **28**, 1537–1545 (2008).

92. S. A. Austin, M. A. Sens, C. K. Combs, Amyloid precursor protein mediates a tyrosine kinase-dependent activation response in endothelial cells. *J. Neurosci.* **29**, 14451–14462 (2009).

93. J. M. Ramaker, T. L. Swanson, P. F. Copenhaver, Amyloid precursor proteins interact with the heterotrimeric G protein Go in the control of neuronal migration. *J. Neurosci.* **33**, 10165–10181 (2013).

94. C. Hilbich, U. Mönning, C. Grund, C. L. Masters, K. Beyreuther, Amyloid-like properties of peptides flanking the epitope of amyloid precursor protein-specific monoclonal antibody 22C11. *J. Biol. Chem.* **268**, 26571–26577 (1993).

95. S. F. Kash, R. S. Johnson, L. H. Tecott, J. L. Noebels, R. D. Mayfield, D. Hanahan, S. Baekkeskov, Epilepsy in mice deficient in the 65-kDa isoform of glutamic acid decarboxylase. *Proc. Natl. Acad. Sci. U.S.A.* **94**, 14060–14065 (1997).

96. M. G. Erlander, N. J. Tillakaratne, S. Feldblum, N. Patel, A. J. Tobin, Two genes encode distinct glutamate decarboxylases. *Neuron* **7**, 91–100 (1991).

97. S. Feldblum, M. G. Erlander, A. J. Tobin, Different distributions of GAD65 and GAD67 mRNAs suggest that the two glutamate decarboxylases play distinctive functional roles. *J. Neurosci. Res.* **34**, 689–706 (1993).

98. Y. C. Chang, D. I. Gottlieb, Characterization of the proteins purified with monoclonal antibodies to glutamic acid decarboxylase. *J. Neurosci.* **8**, 2123–2130 (1988).

99. S. D. Blasio, I. M. N. Wortel, D. A. G. van Bladel, L. E. de Vries, T. D.-d. Boer, K. Worah, N. de Haas, S. I. Buschow, I. J. M. de Vries, C. G. Figdor, S. V. Hato, Human CD1c(+) DCs are critical cellular mediators of immune responses induced by immunogenic cell death. *Oncoimmunology* **5**, e1192739 (2016).

100. M. Feng, K. D. Marjon, F. Zhu, R. Weissman-Tsukamoto, A. Levett, K. Sullivan, K. S. Kao, M. Markovic, P. A. Bump, H. M. Jackson, T. S. Choi, J. Chen, A. M. Banuelos, J. Liu, P. Gip, L. Cheng, D. Wang, I. L. Weissman, Programmed cell removal by calreticulin in tissue homeostasis and cancer. *Nat. Commun.* **9**, 3194 (2018).

101. C. W. Chang, C. W. Chiang, J. D. Gaffaney, E. R. Chapman, M. B. Jackson, Lipid-anchored synaptobrevin provides little or no support for exocytosis or liposome fusion. *J. Biol. Chem.* **291**, 2848–2857 (2016).

102. S. Schoch, F. Deák, A. Königstorfer, M. Mozhayeva, Y. Sara, T. C. Südhof, E. T. Kavalali, SNARE function analyzed in synaptobrevin/VAMP knockout mice. *Science* **294**, 1117–1122 (2001).

103. J. N. K. Nyarko, M. O. Quartey, R. M. Heistad, P. R. Pennington, L. J. Poon, K. J. Knudsen, O. Allonby, A. M. el Zawily, A. Freywald, G. Rauw, G. B. Baker, D. D. Mousseau, Glycosylation states of pre- and post-synaptic markers of 5-HT neurons differ with sex and 5-HTTLPR genotype in cortical autopsy samples. *Front. Neurosci.* **12**, 545 (2018).

104. Q. Zhou, A. Yen, G. Rymarczyk, H. Asai, C. Trengrove, N. Aziz, M. T. Kirber, G. Mostoslavsky, T. Ikezu, B. Wolozin, V. M. Bolotina, Impairment of PARK14-dependent Ca(2+) signalling is a novel determinant of Parkinson's disease. *Nat. Commun.* **7**, 10332 (2016).

105. C. I. Maeder, J.-I. Kim, X. Liang, K. Kaganovsky, A. Shen, Q. Li, Z. Li, S. Wang, X. Z. S. Xu, J. B. Li, Y. K. Xiang, J. B. Ding, K. Shen, The THO complex coordinates transcripts for synapse development and dopamine neuron survival. *Cell* **174**, 1436–1449.e20 (2018).

106. J. C. Watts, C. Condello, J. Stohr, A. Oehler, J. Lee, S. J. DeArmond, L. Lannfelt, M. Ingelsson, K. Giles, S. B. Prusiner, Serial propagation of distinct strains of Aβ prions from Alzheimer's disease patients. *Proc. Natl. Acad. Sci. U.S.A.* **111**, 10323–10328 (2014).

107. J. S. Miners, J. C. Palmer, S. Love, Pathophysiology of hypoperfusion of the precuneus in early Alzheimer's disease. *Brain Pathol.* **26**, 533–541 (2016).

108. A. K. Clippinger, S. D'Alton, W. L. Lin, T. F. Gendron, J. Howard, D. R. Borchelt, A. Cannon, Y. Carlomagno, P. Chakrabarty, C. Cook, T. E. Golde, Y. Levites, L. Ranum, P. J. Schultheis, G. Xu, L. Petrucelli, N. Sahara, D. W. Dickson, B. Giasson, J. Lewis, Robust cytoplasmic accumulation of phosphorylated TDP-43 in transgenic models of tauopathy. *Acta Neuropathol.* **126**, 39–50 (2013).

109. W. Luo, F. Dou, A. Rodina, S. Chip, J. Kim, Q. Zhao, K. Moulick, J. Aguirre, N. Wu, P. Greengard, G. Chiosis, Roles of heat-shock protein 90 in maintaining and facilitating the neurodegenerative phenotype in tauopathies. *Proc. Natl. Acad. Sci. U.S.A.* **104**, 9511–9516 (2007).

110. C. A. Colton, M. P. Vitek, D. A. Wink, Q. Xu, V. Cantillana, M. L. Previti, W. E. van Nostrand, J. B. Weinberg, H. Dawson, NO synthase 2 (NOS2) deletion promotes multiple pathologies in a mouse model of Alzheimer's disease. *Proc. Natl. Acad. Sci. U.S.A.* **103**, 12867–12872 (2006).

111. A. Yuan, A. Kumar, C. Peterhoff, K. Duff, R. A. Nixon, Axonal transport rates in vivo are unaffected by tau deletion or overexpression in mice. *J. Neurosci.* **28**, 1682–1687 (2008).

112. N. S. Gandhi, I. Landrieu, C. Byrne, P. Kukic, L. Amniai, F. X. Cantrelle, J. M. Wieruszeski, R. L. Mancera, Y. Jacquot, G. Lippens, A phosphorylation-induced turn defines the Alzheimer's disease AT8 antibody epitope on the tau protein. *Angew. Chem. Int. Ed. Engl.* **54**, 6819–6823 (2015).

113. K. Ando, A. Maruko-Otake, Y. Ohtake, M. Hayashishita, M. Sekiya, K. M. Iijima, Stabilization of microtubule-unbound tau via tau phosphorylation at Ser262/356 by Par-1/MARK contributes to augmentation of AD-related phosphorylation and Aβ42-induced tau toxicity. *PLOS Genet.* **12**, e1005917 (2016).

114. T. Bilousova, M. Melnik, E. Miyoshi, B. L. Gonzalez, W. W. Poon, H. V. Vinters, C. A. Miller, M. M. Corrada, C. Kawas, A. Hatami, R. Albay III, C. Glabe, K. H. Gylys, Apolipoprotein E/Amyloid-

β complex accumulates in alzheimer disease cortical synapses via apolipoprotein E receptors and is enhanced by APOE4. *Am. J. Pathol.* **189**, 1621–1636 (2019).

115. A. McQuade, Y. J. Kang, J. Hasselmann, A. Jairaman, A. Sotelo, M. Coburn, S. K. Shabestari, J. P. Chadarevian, G. Fote, C. H. Tu, E. Danhash, J. Silva, E. Martinez, C. Cotman, G. A. Prieto, L. M. Thompson, J. S. Steffan, I. Smith, H. Davtyan, M. Cahalan, H. Cho, M. Blurton-Jones, Gene expression and functional deficits underlie TREM2-knockout microglia responses in human models of Alzheimer's disease. *Nat. Commun.* **11**, 5370 (2020).

116. S. L. Siedlak, Y. Jiang, M. L. Huntley, L. Wang, J. Gao, F. Xie, J. Liu, B. Su, G. Perry, X. Wang, TMEM230 accumulation in granulovacuolar degeneration bodies and dystrophic neurites of Alzheimer's disease. *J. Alzheimers Dis.* **58**, 1027–1033 (2017).

117. P. Davies, K. M. Hinkle, N. N. Sukar, B. Sepulveda, R. Mesias, G. Serrano, D. R. Alessi, T. G. Beach, D. L. Benson, C. L. White III, R. M. Cowell, S. S. Das, A. B. West, H. L. Melrose, Comprehensive characterization and optimization of anti-LRRK2 (leucine-rich repeat kinase 2) monoclonal antibodies. *Biochem. J.* **453**, 101–113 (2013).

118. E. J. Bae, N. Y. Yang, M. Song, C. S. Lee, J. S. Lee, B. C. Jung, H. J. Lee, S. Kim, E. Masliah, S. P. Sardi, S. J. Lee, Glucocerebrosidase depletion enhances cell-to-cell transmission of α-synuclein. *Nat. Commun.* **5**, 4755 (2014).

119. S. P. Tay, C. W. S. Yeo, C. Chai, P. J. Chua, H. M. Tan, A. X. Y. Ang, D. L. H. Yip, J. X. Sung, P. H. Tan, B. H. Bay, S. H. Wong, C. Tang, J. M. M. Tan, K. L. Lim, Parkin enhances the expression of cyclin-dependent kinase 6 and negatively regulates the proliferation of breast cancer cells. *J. Biol. Chem.* **285**, 29231–29238 (2010).

120. J. W. Jin, X. Fan, E. del Cid-Pellitero, X. X. Liu, L. Zhou, C. Dai, E. Gibbs, W. He, H. Li, X. Wu, A. Hill, B. R. Leavitt, N. Cashman, L. Liu, J. Lu, T. M. Durcan, Z. Dong, E. A. Fon, Y. T. Wang, Development of an α-synuclein knockdown peptide and evaluation of its efficacy in Parkinson's disease models. *Commun. Biol.* **4**, 232 (2021).

121. Y. Ruan, K. Hu, H. Chen, Autophagy inhibition enhances isorhamnetin-induced mitochondria-dependent apoptosis in non-small cell lung cancer cells. *Mol. Med. Rep.* **12**, 5796–5806 (2015).

122. J. P. Gaut, J. Byun, H. D. Tran, W. M. Lauber, J. A. Carroll, R. S. Hotchkiss, A. Belaaouaj, J. W. Heinecke, Myeloperoxidase produces nitrating oxidants in vivo. *J. Clin. Invest.* **109**, 1311–1319 (2002).

123. M. Dhiman, E. S. Nakayasu, Y. H. Madaiah, B. K. Reynolds, J. J. Wen, I. C. Almeida, N. J. Garg, Enhanced nitrosative stress during Trypanosoma cruzi infection causes nitrotyrosine modification of host proteins: Implications in Chagas' disease. *Am. J. Pathol.* **173**, 728–740 (2008).

124. A. Venkatesan, L. Uzasci, Z. Chen, L. Rajbhandari, C. Anderson, M. H. Lee, M. A. Bianchet, R. Cotter, H. Song, A. Nath, Impairment of adult hippocampal neural progenitor proliferation by methamphetamine: Role for nitrotyrosination. *Mol. Brain* **4**, 28 (2011).

125. K. Newton, M. L. Matsumoto, I. E. Wertz, D. S. Kirkpatrick, J. R. Lill, J. Tan, D. Dugger, N. Gordon, S. S. Sidhu, F. A. Fellouse, L. Komuves, D. M. French, R. E. Ferrando, C. Lam, D. Compaan, C. Yu, I. Bosanac, S. G. Hymowitz, R. F. Kelley, V. M. Dixit, Ubiquitin chain editing revealed by polyubiquitin linkage-specific antibodies. *Cell* **134**, 668–678 (2008).

126. J. V. Ferreira, A. R. Soares, J. S. Ramalho, P. Pereira, H. Girao, K63 linked ubiquitin chain formation is a signal for HIF1A degradation by chaperone-mediated autophagy. *Sci. Rep.* **5**, 10210 (2015).

127. M. H. Chen, T. L. Hagemann, R. A. Quinlan, A. Messing, M. D. Perng, Caspase cleavage of GFAP produces an assembly-compromised proteolytic fragment that promotes filament aggregation. *ASN Neuro* **5**, e00125 (2013).

128. Y. S. Chen, S. C. Lim, M. H. Chen, R. A. Quinlan, M. D. Perng, Alexander disease causing mutations in the C-terminal domain of GFAP are deleterious both to assembly and network formation with the potential to both activate caspase 3 and decrease cell viability. *Exp. Cell Res.* **317**, 2252–2266 (2011).

129. S. A. Baker, C. R. Gajera, A. M. Wawro, M. R. Corces, T. J. Montine, GATM and GAMT synthesize creatine locally throughout the mammalian body and within oligodendrocytes of the brain. *Brain Res.* **1770**, 147627 (2021).

130. A. M. Wawro, C. R. Gajera, S. A. Baker, J. J. Nirschl, H. Vogel, T. J. Montine, Creatine transport and pathological changes in creatine transporter deficient mice. *J. Inherit. Metab. Dis.* **44**, 939–948 (2021).